JOURNAL OF GEOPHYSICAL RESEARCH, VOL. 104, NO. A7, PAGES 14,717–14,727, JULY 1, 1999

A Pc5 ULF wave with large azimuthal wavenumber observed within the morning sector plasmasphere by Sub-Auroral Magnetometer Network

G. Chisham[1]

Astronomy Unit, Queen Mary and Westfield College, London, England, United Kingdom

I. R. Mann

Department of Physics, University of York, York, England, United Kingdom

Abstract. In this paper we present details of an unusual Pc5 ULF wave with a large azimuthal wavenumber (m) which is observed within the plasmasphere by ground-based magnetometers. In a previous statistical study, 129 Pc5 events were identified at midlatitudes by the U.K. Sub-Auroral Magnetometer Network (SAMNET), but only three displayed large azimuthal wavenumbers ($m > 10$). Analysis of the variation of wave parameters during one of these events using a novel complex demodulation technique is presented. The technique reveals the temporal variation of wave characteristics, including the azimuthal wavenumber and wave frequency, and allows us to study the azimuthal dispersion characteristics of the wave and estimate the azimuthal phase and group speeds. The method used to estimate the azimuthal wavenumbers resolves the ambiguity resulting from aliasing, which can occur for large-m waves observed at stations more than one azimuthal wavelength apart. The drift-bounce resonance mechanism is discussed as a possible wave excitation mechanism for this event, and resonance with H^+ and/or O^+ ions at the inner edge of the ring current is presented as a possible excitation scenario.

1. Introduction

The azimuthal wavenumbers (m values) of magnetospheric ULF waves are useful diagnostics of the wave generation mechanisms. They can provide important information about the azimuthal scale and propagation direction of a wave. Field line guided Alfvén waves in the magnetosphere are dominantly small-m ($\sim 0-5$) toroidal field line resonances (FLRs) [*Southwood*, 1974; *Chen and Hasegawa*, 1974] with periods in the Pc4-Pc5 range (45-600 s). These FLRs are thought to be predominantly driven by energy transfer from compressional modes; magnetospheric waveguide modes [e.g., *Mann et al.*, 1998], cavity modes [e.g., *Kivelson and Southwood*, 1985, 1986], and the Kelvin-Helmholtz instability at the magnetopause boundary [e.g., *Pu and Kivelson*, 1983] are possible candidates, and all have their energy source in the solar wind. FLRs are dominated in space by magnetic perturbations in the azimuthal direction [e.g., *Kokubun et al.*, 1989] and on the ground by magnetic perturbations in the north-south direction [e.g., *Samson*, 1972] which results from the 90° rotation of an Alfvén wave signal on transmission through the ionosphere [e.g., *Hughes*, 1974; *Hughes and Southwood*, 1976a, b]. However, there are also a large number of magnetospheric Pc4-Pc5 waves which are characterized by larger m values (> 10). These waves are often guided poloidal Alfvén resonances being dominated in space by magnetic perturbations in the radial direction [e.g., *Takahashi et al.*, 1990] and on the ground by magnetic perturbations in the east-west direction [e.g., *Chisham et al.*, 1997], although a dominant compressional component in the magnetosphere can also be a feature of some large-m waves [e.g., *Takahashi et al.*, 1985]. For large-m waves, wave growth is thought to occur through wave-particle interactions with energetic particle sources inside the magnetosphere. They do not result from external solar wind sources as with small-m Pc4-Pc5 waves.

Three types of large-m waves have been well documented. Radially polarized second-harmonic waves,

[1]Now at British Antarctic Survey, Natural Environment Research Council, Cambridge, England, United Kingdom.

Paper number 1999JA900147.
0148-0227/99/1999JA900147$09.00

typically in the Pc4 period range, are regularly observed by spacecraft [e.g., *Arthur and McPherron*, 1981; *Hughes and Grard*, 1984], with an occurrence distribution that peaks in the afternoon sector of the magnetosphere [*Anderson et al.*, 1990]. Multiple spacecraft observations of these waves [e.g., *Hughes et al.*, 1978, 1979] have established that they are westward propagating waves with $|m| \sim 100$. The small azimuthal scale of waves with such large m results in them being shielded from the ground [*Hughes and Southwood*, 1976a], and hence these events are not observed by ground-based magnetometers. "Giant pulsations" (Pgs) are also waves in the Pc4 period range but display differences from those described above. They are observed predominantly on the ground and preferentially in the early morning sector of the magnetosphere [e.g., *Chisham et al.*, 1997, and references therein]. Typical m values for Pgs, as measured by longitudinally spaced ground magnetometer stations, are $\sim 20 - 40$ [e.g., *Chisham et al.*, 1992]. These smaller m values are the reason that these waves are observable on the ground. Simultaneous ground-satellite observations of Pgs are rare [e.g., *Hillebrand et al.*, 1982; *Takahashi et al.*, 1992], and a widely accepted theory of their generation has not emerged owing to the uncertainty regarding their standing wave mode. Large-m waves in the Pc5 range are most often of the type termed "storm-time Pc5" [e.g., *Barfield et al.*, 1972; *Barfield and McPherron*, 1972; *Walker et al.*, 1982] or "compressional Pc5" [e.g., *Takahashi et al.*, 1985]. Typically, these are large-amplitude waves, observed by spacecraft during disturbed times, often during the main phase of a magnetic storm. They have a peak occurrence around dusk and often have compressional components which are comparable to the transverse ones. These waves most likely have their energy source in the ring current; compressional Pc5 waves have been observed to propagate westward with speeds matching 10-100 keV proton drift speeds. Similar large-m Pc5 events have been observed in the local afternoon by auroral radar and ground magnetometers [e.g., *Allan et al.*, 1982, 1983; *Walker et al.*, 1982]. These events are westward propagating with m values ~ 35. A modified drift-mirror instability [*Walker et al.*, 1982] has been suggested as a generation mechanism for these events.

The estimation of m values requires longitudinally or azimuthally spaced coherent wave observations. To measure large m values, the azimuthal separation must be small (less than $2\pi/m$ rad). An ambiguity occurs in the m value estimation if measurements are made more than one azimuthal wavelength apart. It is particularly difficult to measure large m values using azimuthally spaced satellites, and only a few such observations exist [e.g., *Hughes et al.*, 1978, 1979; *Takahashi et al.*, 1985]. It is, however, possible to estimate m values with data from a single spacecraft using the "finite Larmor radius effect" [e.g., *Lin et al.*, 1988], which uses back-to-back particle detectors. Estimating m values using ground-based radar and magnetometers is easier. Large-m waves have been observed by coherent radar in a number of studies, both storm-time Pc5 [e.g., *Allan et al.*, 1982, 1983; *Grant et al.*, 1992] and Pgs [e.g., *Poulter et al.*, 1983; *Chisham et al.*, 1992]. On the ground, only waves with $|m| < 50$ can generally be observed by magnetometers owing to ionospheric shielding effects. Hence ground observations of large-m waves have been limited to a small number of Pgs [e.g., *Chisham et al.*, 1990, 1992] and storm-time Pc5 [e.g., *Allan et al.*, 1983]. These waves are typically observed within the auroral zone. Pc4-Pc5 waves with large m values are rarely observed at lower latitudes and inside the plasmasphere. One possible exception is a series of Pgs observed on three successive days by *Green* [1985]. These Pgs were observed within the plasmasphere, one being resonant at $L \sim 2.8$. However, no m-value estimations were made for these events.

In this paper we present observations of a large-m Pc5 made by the United Kingdom Sub-Auroral Magnetometer Network (SAMNET) within the plasmasphere. Using the technique of complex demodulation, the temporal variation of the wave frequency and m value have been determined in order to study the azimuthal dispersion characteristics of the wave. The possible generation mechanisms responsible for this wave are discussed.

2. Data Analysis

2.1. Instrumentation

At the time of the Pc5 observation, SAMNET [*Yeoman et al.*, 1990] comprised seven three-component fluxgate magnetometers with a sampling period of 5 s. SAMNET data are recorded in the H (geomagnetic north-south), D (geomagnetic east-west), and Z (vertical) coordinate system. The SAMNET magnetometers measure magnetic field variations over a range of ± 512 nT with a resolution of 0.25 nT. SAMNET is a two-dimensional magnetometer array which originally consisted of two longitudinal chains (at $L \sim 4.4$ and $L \sim 3.3$) and a latitudinal chain (on the United Kingdom meridian). The geographic and corrected geomagnetic coordinates of the seven SAMNET stations used in this study are presented in Table 1 along with their dipole-field L-shell position.

2.2. Event Selection

In over a year of SAMNET data, 129 Pc5 wave events were identified in data from 1988-1989 [*Chisham and Orr*, 1997] using the following selection criteria: (1) The wave consisted of at least three wave cycles, with a stable period in the Pc5 range (150 - 600 s); (2) the wave amplitude was at least 3 nT peak to peak; and (3) the wave was visible at all the available stations on the SAMNET array. Of the 129 Pc5 events observed, for only three was $m > 10$. The small number of events with large m values may be partially a

Table 1. Coordinates and L-Shell Values of the SAMNET Stations

Station	Code	Geographic		Geomagnetic		L Shell
		Latitude, deg	Longitude, deg	Latitude, deg	Longitude, deg	
Faroes	FAR	62.05	352.98	60.77	78.12	4.26
Nordli	NOR	64.37	13.36	61.28	95.28	4.40
Oulu	OUL	65.10	25.85	61.30	105.56	4.41
Glenmore	GML	57.16	356.32	54.94	77.99	3.08
Kvistaberg	KVI	59.50	17.63	55.83	95.95	3.22
Nurmijarvi	NUR	60.51	24.66	56.59	102.17	3.35
York	YOR	53.95	358.95	50.99	78.57	2.57

All values were calculated by using the International Geomagnetic Reference Field for 1988 at an altitude of 120 km. SAMNET, the U.K. Sub-Auroral Magnetometer Network.

consequence of the selection criteria. Waves with large m values are often longitudinally (and latitudinally) localized and hence would not always be observable over the complete longitudinal extent of SAMNET (~27°). One of the three events which was observed at all the SAMNET stations is studied in further detail here.

The event occurred on May 13, 1988, in the morning sector of the magnetosphere. Figure 1 presents unfiltered SAMNET magnetograms of the H component (Figure 1a) and the D component (Figure 1b) of the ground magnetic field. The Pc5 occurs between ~0630 and 0740 UT and is almost sinusoidal at some stations. The wave period is ~ 200 s. The wave amplitude appears greater both in the D component and on the lower latitude SAMNET longitudinal chain (Glenmore (GML), Kvistaberg (KVI), and Nurmijarvi (NUR)), which is generally located within the plasmasphere. The plasmapause position during this event has been estimated using the method of *Yeoman* [1988], which is based on that of *Orr and Webb* [1975]. This method places the plasmapause, at the local time of the SAMNET stations, in the range $L \sim 4.5 - 5.0$, which is

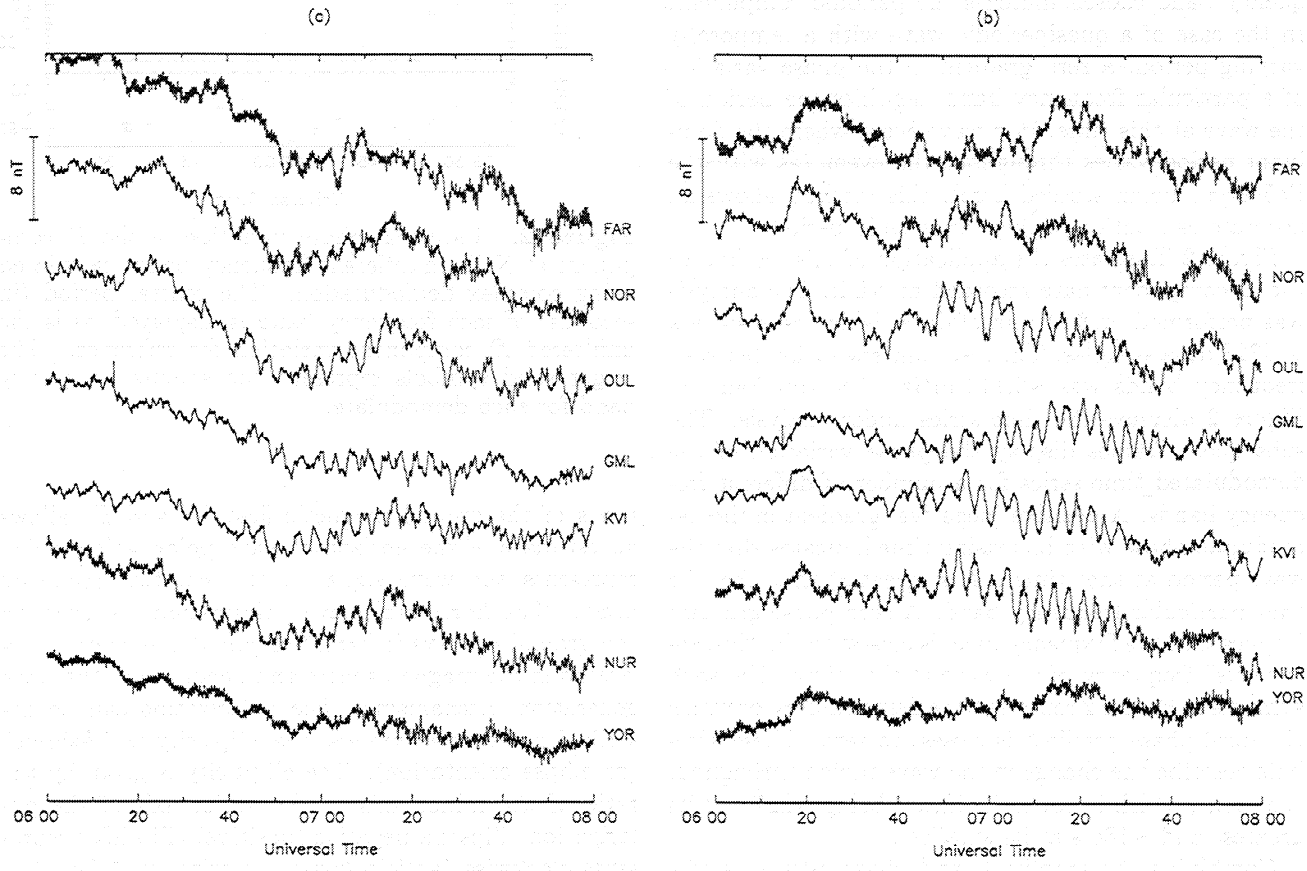

Figure 1. Unfiltered magnetograms from May 13, 1988, for the (a) H component of the magnetic field and (b) D component of the magnetic field. See Table 1 for station details.

just poleward of the higher latitude SAMNET longitudinal chain. The lower latitude chain is well within the plasmasphere.

2.3. Complex Demodulation

Complex demodulation [*Bingham et al.*, 1967] is a time series analysis technique which allows an estimation of the temporal variation of the amplitude and phase of selected frequency components of a time series. It provides "instantaneous" or "time-local" properties which make it an ideal tool for studying nonstationary time series which may exhibit frequency dispersion. Using this method, the frequency modulation of the wave signal can be distinguished from the amplitude modulation of the signal. The technique was first applied to geomagnetic data by *Banks* [1975] and later to ULF wave variations by *Beamish et al.* [1979] and *Hanson et al.* [1979].

When studying ULF wave events the "instantaneous" period (or frequency) of the event can be determined by studying the phase variation of a number of demodulated time series representing different frequency bands. Only a discrete number of frequency bands can be studied since the analysis involves applying a fast Fourier transform to a finite time series. If a time series contains a strictly periodic component, then the phase of the demodulated time series will vary linearly with time; the gradient in this phase variation will be zero if the frequency band chosen matches the periodic component. In the case of a quasiperiodic wave with a temporally varying period, a zero gradient in the phase variation of a particular frequency band identifies the period of the wave at this time. In a wave event where the dominant period varies throughout the event (as with the Pc5 event being studied here), this method allows an accurate estimation of this variation in period.

Figure 2 illustrates the application of this method to the D component data recorded at NUR. The analysis was performed on 144 min of data, which corresponds to 1728 data samples. The resultant resolution between frequency bands was ~0.116 mHz. The top frame in Figure 2 displays the time series under analysis. The subsequent frames display the phase variation of the demodulated time series for a number of different frequency bands. A positive (negative) gradient in the demodulate phase with increasing time indicates that the wave period at that time is less (greater) than that for that particular frequency band. A zero phase gradient implies that the frequency band is closest to the "instantaneous" frequency of the wave at that time. The solid symbols in Figure 2 represent the demodulates for which the local phase gradient is closest to zero. These symbols describe the change in the wave period throughout the event, which is not insignificant being ~227 s at its greatest and ~184 s at its smallest.

Combining the amplitude and phase estimates of a particular demodulate from the two horizontal components of the ground magnetic field (H and D) allows an estimate of the horizontal wave polarization which represents the wave signal in the selected frequency band. The horizontal wave polarization observed on the ground conveys information about the wave polarization in the magnetosphere and hence about the wave generation mechanisms. The polarization can be described by two parameters, the ellipticity and azimuth (or ellipse orientation). The ellipticity is given by the ratio of the minor axis to the major axis of the polarization ellipse; a negative (positive) ellipticity represents clockwise (anticlockwise) polarization (viewed in the direction of the geomagnetic field line). The po-

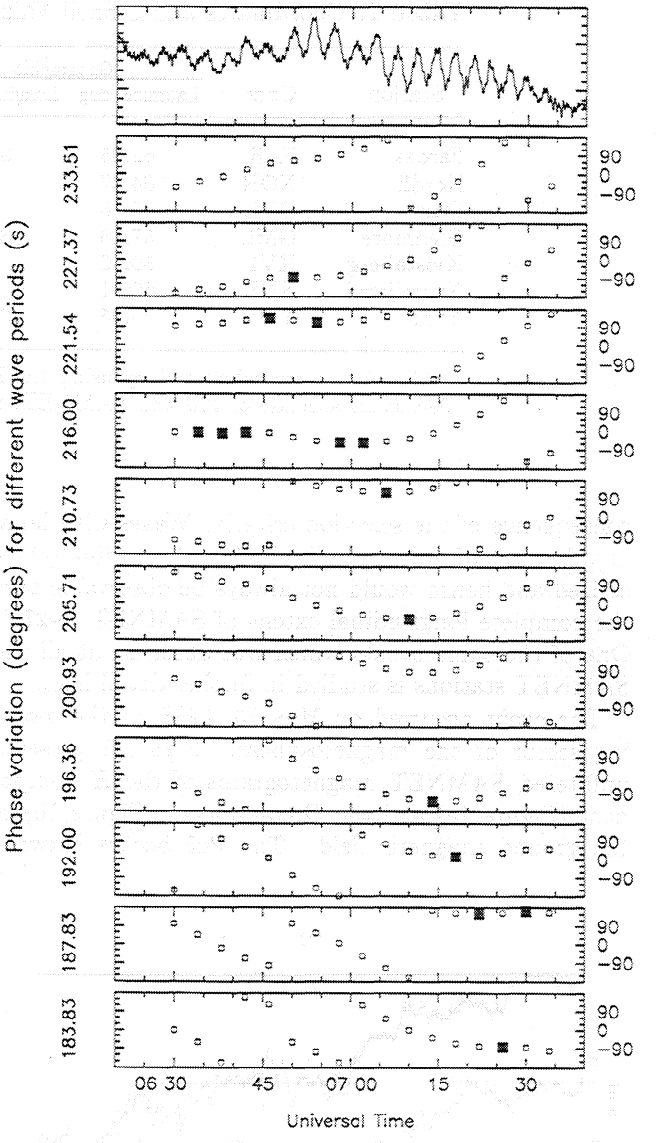

Figure 2. Temporal phase variation of the D component at NUR in different frequency bands calculated using complex demodulation. The central period (in seconds) of each frequency band is displayed, as is the unfiltered D component variation for reference. The larger solid symbols represent the selected frequency band for each demodulate.

Table 2. Geomagnetic Longitude Differences and Maximum Unambiguous Azimuthal Wavenumbers for the Six SAMNET Station Pairs

Station Pair	$\Delta\lambda$	$\lvert m_1\rvert$	$\lvert m_2\rvert$
FAR - NOR	17.16	10.5	21.0
FAR - OUL	27.44	6.6	13.1
NOR - OUL	10.28	17.5	35.0
GML - KVI	17.96	10.0	20.0
GML - NUR	24.18	7.4	14.9
KVI - NUR	6.22	28.9	57.9

larization azimuth is 0° for a north-south orientation and increases positively as the polarization orientation rotates clockwise, being 90° for an east-west orientation. The polarization characteristics of a wave at a particular time (for a particular frequency band) can be presented in the form of two-dimensional polarization maps, which illustrate the horizontal polarization variation across the SAMNET array.

2.4. Determination of m Values

Using the wave phase differences observed between stations on the two SAMNET longitudinal chains, a total of six m value estimates can usually be made for each demodulate during an event (for the following station pairs: FAR-NOR, FAR-OUL, NOR-OUL, GML-KVI, GML-NUR, and KVI-NUR). The stations in each pair occupy very similar geomagnetic latitudes, and so any latitudinal phase variations produce only small errors in m. To minimize this error, the m values are calculated using differences in the D component phase only as the H component phase generally shows more variability with latitude (especially in the vicinity of FLRs). The m value is given by

$$m = \frac{\Delta\phi}{\Delta\lambda} \tag{1}$$

where $\Delta\phi$ is the D component phase difference between the two stations and $\Delta\lambda$ is their geomagnetic longitude difference. The differences in geomagnetic longitude for each of the station pairs are shown in Table 2. Positive (negative) m values represent waves with eastward (westward) phase propagation.

In cases where two stations have a large longitudinal separation, an ambiguity in the m value can occur for ULF wave events with large m values. If the phase difference between two stations is greater than 180° (or 360° if the direction of phase propagation is known), then it is impossible to unambiguously determine the associated m value using (1). The maximum m values that can be measured for each station pair without the occurrence of an ambiguity are displayed in Table 2; the value $|m_1|$ represents the maximum m value that can be estimated when the direction of phase propagation is not known, whereas $|m_2|$ represents the maximum m value that can be estimated when the direction of phase propagation is known. Table 2 shows that m values up to $|m| \sim 10$ can be measured with confidence. Determining an optimum station separation for the best estimation of m values is difficult. A small separation clearly identifies large m values, but the estimation of small m values can be unreliable owing to the small phase differences involved. A large separation allows an accurate determination of small m values, but an ambiguity occurs for waves with large m values. For the majority of Pc5 events observed by SAMNET, $|m| \sim 1-5$ [*Chisham and Orr*, 1997], and so there is no problem with an ambiguity in the m value estimation. Larger m values ($|m| > 10$) can be measured between KVI and NUR owing to the smaller longitudinal separation (up to $|m| \sim 29$ or $|m| \sim 58$ depending on whether the direction of phase propagation is known). If $|m| > 10$ is

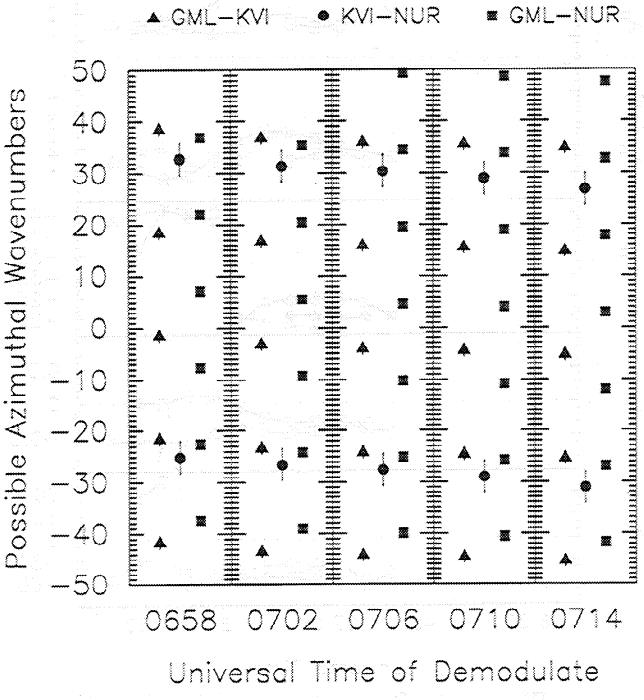

Figure 3. The range of possible azimuthal wavenumbers that can be estimated from the phase differences between the three stations on the lower latitude SAMNET chain for five consecutive demodulates.

measured between KVI and NUR, the m values measured between the other station pairs may be erroneous, and so a method is needed to determine the correct m values.

To correctly determine an m value suspected of being large, we compare all the possible m values estimated from the three phase differences between the three station pairs on a SAMNET longitudinal chain as given by

$$m = \frac{\Delta\phi + 2\pi N}{\Delta\lambda} \tag{2}$$

where N is an integer. Figure 3 presents possible m values for five consecutive demodulates of data from the lower latitude SAMNET chain. The m values are restricted to $m = \pm 50$, which represents the probable extent of the modes that can be observed on the ground. The errors in m are a result of the uncertainty in the phase measurements made at each station. Some of this uncertainty is a result of timing errors between stations; the maximum timing error expected between any two SAMNET stations is ~2 s. For wave periods ~200 s this results in a phase uncertainty ~4°. For waves with large m this uncertainty is generally a small fraction of the phase difference between the stations.

Figure 3 shows that the station pair KVI-NUR has the fewest estimates of m (and the largest error) owing to the small longitudinal separation. For the 0658 UT demodulate all three station pairings suggest possible m values around $m \sim -23$ and $m \sim 36$. The waveforms (Figure 1) indicate that this particular wave event (as seen on the lower latitude SAMNET chain) is westward propagating (NUR observes the event first), and so those values of $m \sim -23$ represent the best estimates of the azimuthal wavenumber at this time. Using (1) without considering the ambiguity would have led to estimates of m for the station pairs GML-KVI and GML-NUR of $m \sim -2$ and $m \sim -8$, respectively. This would have been obviously erroneous. The other demodulates shown in Figure 3 illustrate the reliability of the method and show the slow variation that occurs in

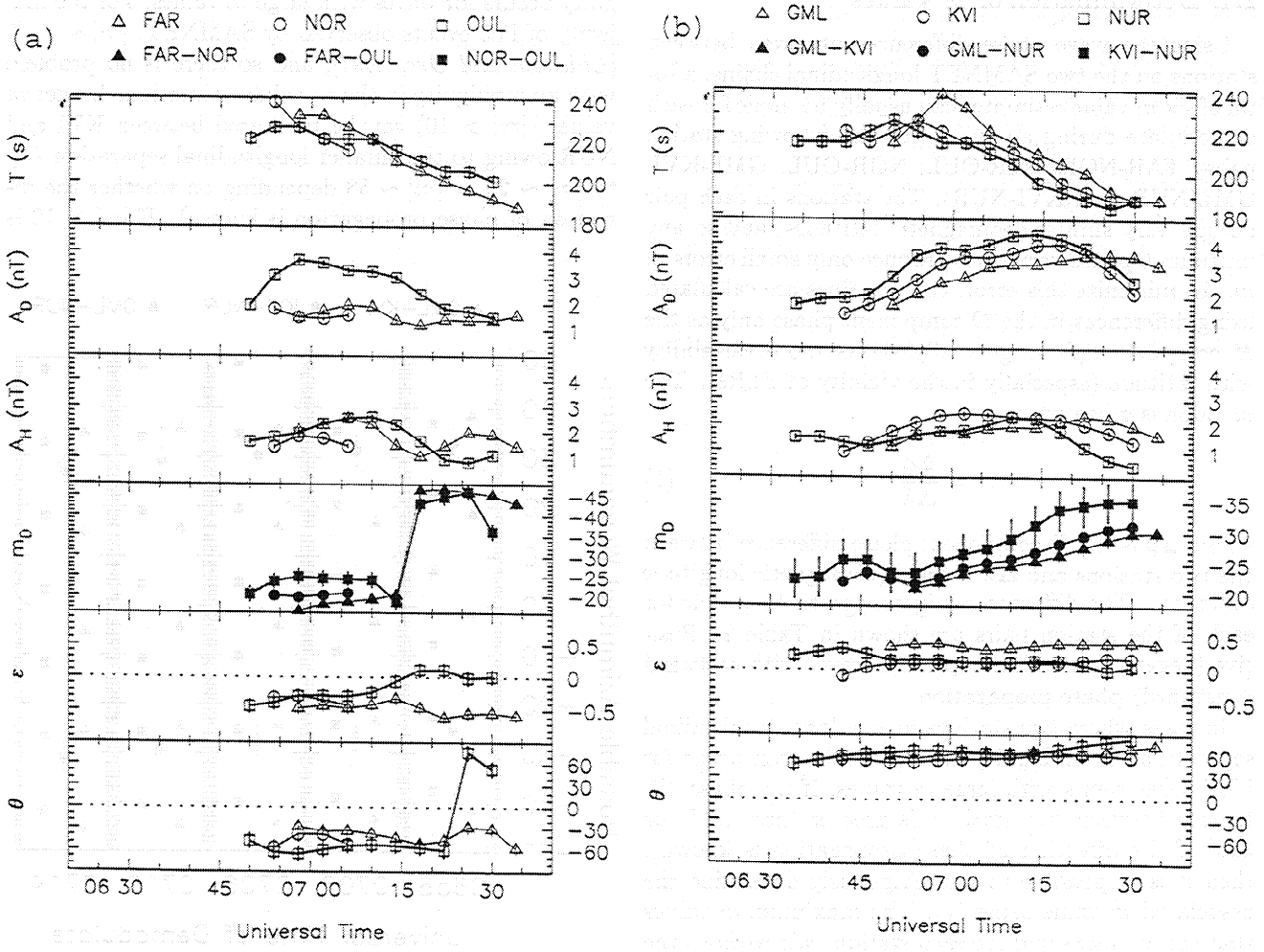

Figure 4. Parameters resulting from the complex demodulation analysis of data from (a) the higher latitude SAMNET longitudinal chain and (b) the lower latitude SAMNET longitudinal chain. Consecutive frames from the top display the central wave period of the selected frequency band, the D component wave amplitude, the H component wave amplitude, the D component azimuthal wavenumber, the polarization ellipticity, and the polarization azimuth.

m with time. Using this method, accurate m values can be calculated for any SAMNET Pc5 events which may have large m values.

2.5. Temporal Profiles of Event Characteristics

The results of the complex demodulation analysis for this event are presented in Figure 4. Figure 4 presents the temporal variations of the estimated wave period T, the D component wave amplitude A_D, the H component wave amplitude A_H, the azimuthal wavenumber m_D, the horizontal polarization ellipticity ε, and azimuth θ for the higher latitude (Figure 4a) and lower latitude (Figure 4b) SAMNET longitudinal chains. Poor coverage of the event occurred at some stations (particularly those on the higher latitude chain) where the wave power was low in the frequency band of interest.

After an initial rise the wave period T on both longitudinal chains shows a steady decrease from $\sim 220-240$ s to $\sim 180-190$ s. On the lower latitude chain this decrease in period occurs at the easternmost station (NUR) first and finally at the westernmost station (GML) $\sim 8(\pm 2)$ min later. This change in period is not simply a local time effect. These two stations are separated by $\sim 24°$ in longitude, which represents a local time difference ~ 96 min. For this change in period to represent purely a local time effect a 96 min delay would be expected between similar wave periods at NUR and GML. The shorter delay observed suggests that the wave disturbance on the lower latitude chain is propagating westward at $\sim 8.1(\pm 2.9) \times 10^{-4}$ rad/s. On the higher latitude chain this westward propagation is not apparent.

On both chains the wave amplitude is generally dominant in the D component (typically $A_D \sim 2A_H$), and the wave amplitude is generally greater on the lower latitude chain. Hence the wave amplitude maximum is located well within the plasmasphere. As with the period variation, the peaks in the lower latitude chain D component amplitude variation occur first at the easternmost station (NUR) and last at the westernmost station (GML). The time delay measured from the amplitude variations is $\sim 12(\pm 2)$ min, which suggests that the wave disturbance is propagating westward at $\sim 5.1(\pm 1.2) \times 10^{-4}$ rad/s. Again, on the higher latitude chain this westward propagation is not apparent. The data even suggest that the wave disturbance may be propagating eastward on the higher latitude chain. However, this may just be a result of the reduced wave signal on the higher latitude chain producing unreliable estimates of wave period and amplitude. The differences between the two chains highlight the latitudinal localization of the event which is typical of guided poloidal wave modes [e.g., *Chisham et al.*, 1997].

The variation in the azimuthal wavenumber m_D is also different on the two chains. On the lower latitude chain, m_D is negative (representing westward phase propagation) and rises steadily in magnitude from ~ -21 to ~ -30 between GML and KVI and from ~ -23 to ~ -35 between KVI and NUR. These differences may suggest an azimuthal variation in m as well as a temporal one. On the higher latitude chain, m_D is also negative but stays constant at ~ -20 before jumping to ~ -45 at around 0715 UT. The wave amplitude at some of the higher latitude stations (especially NOR) is very small across some of this interval, and hence the higher latitude chain m values may not be wholly reliable. Both chains, however, do show the existence of waves with large m within the plasmasphere.

The wave polarization characteristics are distinctly different on the two chains. The polarization ellipticity on the higher latitude chain is predominantly negative (representing clockwise polarization), whereas the ellipticity on the lower latitude chain, although close to zero at some stations, is predominantly positive (representing anticlockwise polarization). The polarization azimuth (or ellipse orientation) is predominantly negative on the higher latitude chain (representing ellipses approximately oriented in the north-west to south-east direction), whereas the azimuth is positive on the lower latitude chain (representing ellipses approximately oriented in the north-east to south-west direction). Figure 5 shows a snapshot of the wave polarization across the SAMNET array at $\sim$0706 UT which displays polarization features which are typical of the event. The near-linear polarization at NUR suggests that this may be close to a resonance position. The polarization variation with latitude is identical to that observed for Pgs either side of a resonance position [*Chisham et al.*, 1997]. It seems likely that this latitudinal polarization variation, along with the typically observed large m values and dominant D component (radial in the magnetosphere)

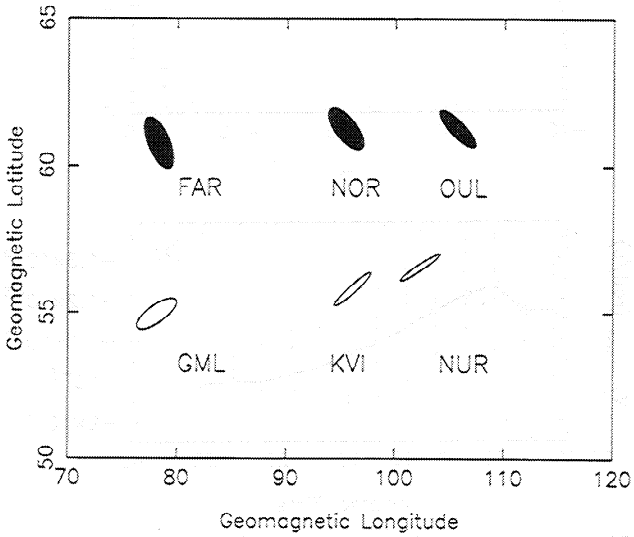

Figure 5. Snapshot of the Pc5 polarization across the SAMNET array for the demodulate located at 0706 UT. The solid ellipses represent clockwise polarization, whereas the open ellipses represent anticlockwise polarization.

amplitudes, is a characteristic of guided poloidal resonances.

2.6. Azimuthal Wave Dispersion Characteristics

Figure 6 presents the azimuthal dispersion characteristics of the large-m Pc5 event as measured at KVI. Figure 6a displays the dispersion relation between the wave frequency ω and the azimuthal wavenumber m. The m values at KVI were estimated by linearly interpolating between those measured using the station pairs GML-KVI and KVI-NUR, assuming that these m values represented the value at the midpoint in longitude between the two stations. Figure 6a shows that the wave frequency increases approximately linearly with $|m|$. The dashed line (marked B in Figure 6a) represents a least squares fit to the data and corresponds to an azimuthal group speed $V_{\phi-\text{group}} \sim -5.0\times10^{-4}$ rad/s. This compares extremely well with that estimated from the delays in the lower latitude chain period and amplitude variations detailed in section 2.5. The dotted lines (marked A and C in Figure 6a) represent the limits of possible azimuthal group speeds considering the errors in the estimations of m and ω. Line A corresponds to $V_{\phi-\text{group}} \sim -3.5 \times 10^{-4}$ rad/s, whereas line C corresponds to $V_{\phi-\text{group}} \sim -12.0 \times 10^{-4}$ rad/s. The azimuthal group velocities estimated from the delays detailed in section 2.5 are well within this range.

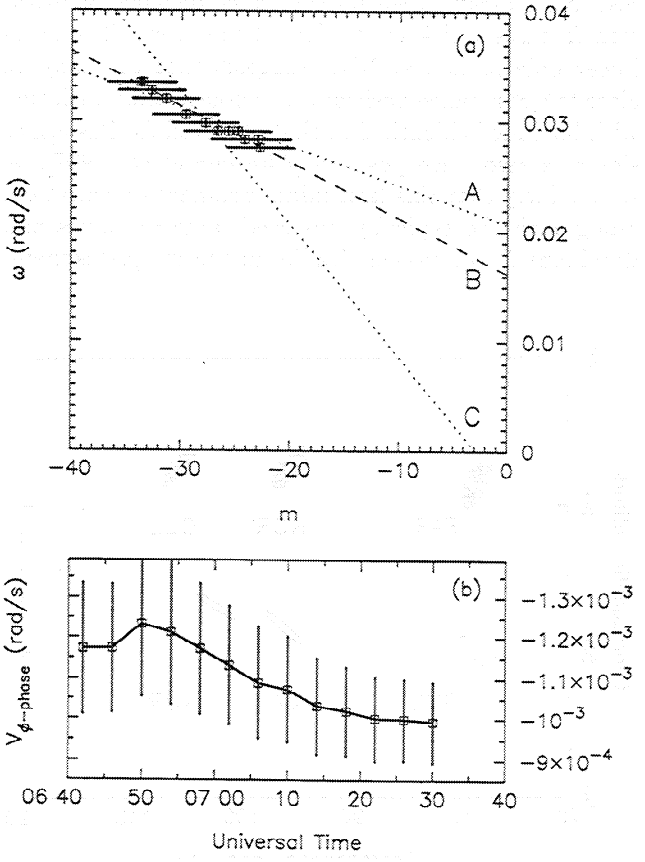

Figure 6. Azimuthal dispersion characteristics at KVI, including (a) the azimuthal dispersion relation between the wave frequency and azimuthal wavenumber and (b) the azimuthal phase speed variation through the event. The dashed lines represent different azimuthal group speeds.

Figure 6b presents the variation of the azimuthal phase speed $V_{\phi-\text{phase}}$ with time. Although the phase speed falls slightly during the event, it is approximately constant; the errors in the estimations are large enough to allow both positive and negative gradients to be drawn through the points. Large-m waves displaying a constant westward azimuthal phase speed have been observed before with auroral radar [*Allan et al.*, 1982, 1983]. These studies presented a large-m Pc5 event for which the m value and period varied so as to keep the azimuthal phase speed approximately constant, which was interpreted as resulting from a drift instability with ring current protons traveling at the azimuthal phase speed.

3. Discussion

This study presents ground-based magnetometer observations of a large-m Pc5 ULF wave within the plasmasphere which (to our knowledge) is unique to the literature. This Pc5 does not fall into the categories of the storm-time Pc5 or the afternoon-sector poloidal Pc4. It has some characteristics which are similar to Pgs, but this Pc5 is resonant at a much lower latitude than typical Pg resonances, and its period is longer.

Large-m waves typically gain energy from wave-particle interactions with unstable particle populations within the magnetosphere. Both the K_p index ($\sim$ 1− to 2−) and the D_{st} index (~ -5 to -15 nT) are low in the 24 hour period preceding the event. These conditions describe an extended period of geomagnetic quiet and a reduced ring current. The A_E index (not shown), whilst predominantly quiet, does show the occurrence of isolated substorms at ~0200 UT on May 12, 1988, and ~0230 UT on May 13, 1988. The particle injections associated with these substorms could provide the particle populations to feed an instability. A number of instabilities that can be responsible for wave growth can be ruled out. Although this event occurred near the inner edge of the ring current (typically $L \sim 3-4$), the plasmasphere is generally a region of very cold plasma, with $\beta \ll 1$. Therefore instabilities that require large β, such as the drift-mirror instability [*Hasegawa*, 1969], appear unlikely driving mechanisms for this event.

A possible mechanism for wave growth is the drift-bounce resonance instability with energetic particles [*Southwood et al.*, 1969; *Southwood*, 1976]. The resonance condition is given by

$$\omega - m\omega_D = N\omega_B \tag{3}$$

where ω_D and ω_B represent the particle drift and bounce frequencies, respectively, and N is an integer.

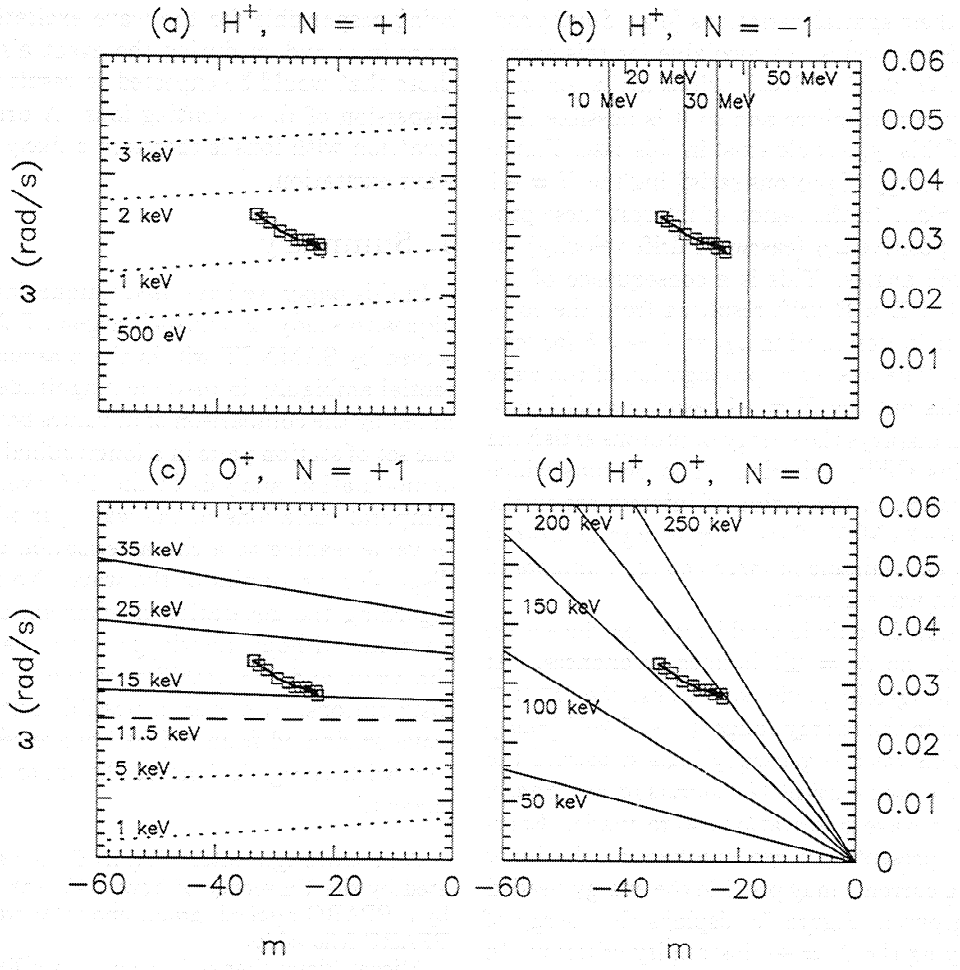

Figure 7. Model ω-m profiles for different energy particles satisfying the drift-bounce resonance criterion for (a) protons, $N = +1$; (b) protons, $N = -1$; (c) O^+ ions, $N = +1$; and (d) all ions, $N = 0$. The square symbols represent the observed ω-m variation as illustrated in Figure 6.

Southwood [1976] showed that the $N = 0, \pm 1$ resonances are dominant in the magnetosphere. The $N = 0$ drift resonance requires the wave to be an odd-mode standing wave (e.g., fundamental), whereas the $N = \pm 1$ bounce resonances typically require the wave to be an even-mode standing wave (e.g., second harmonic). Generally, it is not possible to distinguish whether waves have a fundamental or second-harmonic standing wave structure without either in situ spacecraft measurements in the equatorial plane or conjugate ground-based observations. Neither of these observations were available for this event.

Figure 7 presents examples of model ω-m variations for different drift-bounce resonant interactions with different energy particles to compare with the observed values of ω and m. The model ω-m profiles are calculated from (3); the value of ω_D used is that used by *Chisham* [1996], which includes both an energy dependent gradient-curvature term and electric field dependent convection and corotation terms. All the model ω-m profiles in Figure 7 are labeled with their associated energy, and the calculations have assumed that $K_p = 1-$ (the K_p at the time of the event) and that the pitch angle $\alpha = 20°$. Small changes in K_p result in negligible changes in the ω-m profiles. Changes in the pitch angle result in more significant changes; for example, a change of $\Delta E/E \sim 0.3$ occurs between $\alpha = 0°$ and $\alpha = 90°$ for a particular ω and m. In Figure 7 the squares and the bold line represent the observed ω-m variation (which moves to larger ω and $|m|$ as time increases). the solid lines represent ω-m profiles for which ω_D is negative, the dotted lines represent ω-m profiles for which ω_D is positive, and the dashed line represents the ω-m profile for which ω_D is zero (i.e., the azimuthal contribution of the $\mathbf{E} \times \mathbf{B}$ drifts cancels that of the gradient-curvature drift).

If these waves are second-harmonic standing waves, particles satisfying the $N = \pm 1$ bounce resonance condition will be in resonance with the wave and hence will be able to exchange energy with the wave. Whether the particles provide energy to the wave or vice versa depends on the characteristics of the particle distribution

functions and their spatial variations [e.g., *Southwood*, 1976]. This information is not available for this event. However, unstable particle distributions are a common feature of the magnetosphere and so it is possible that distributions of this type could exist in this case. Figure 7a displays the energy of protons satisfying the $N = +1$ instability criterion. In the region of interest these protons all have a positive ω_D (eastward drift velocity) for all possible pitch angles. This is a consequence of the eastward directed $\mathbf{E} \times \mathbf{B}$ drift resulting from the corotation electric field dominating ω_D at $L \sim 3.5$ for low-energy protons. The westward propagation of the wave disturbance rules out the $N = +1$ resonance with protons. Figure 7b displays the energy of protons satisfying the $N = -1$ instability criterion. The protons which satisfy the criterion in the region of interest are in the energy range 15 - 30 MeV. These very energetic protons are unlikely to be available in large enough numbers to cause significant wave growth.

Protons are not the only ions which can produce wave growth through the $N = \pm 1$ bounce resonances. At $L = 3.5$, in quiet geomagnetic conditions, the O^+/H^+ ratio is $\sim 1-10$ in the energy range $0.1-17$ keV [*Sharp et al.*, 1985]. This ratio is generally highest toward the inner edge of the ring current [*Lennartsson and Sharp*, 1982] where our wave observations were made. Energetic O^+ ions, present in large numbers at the inner edge of the ring current, may provide the energy needed for the wave growth. Figure 7c displays the energy of O^+ ions satisfying the $N = +1$ instability criterion. In the region of interest this requires O^+ ions in the energy range $15 - 20$ keV. O^+ ions with these energies at $L \sim 3-4$ have drift periods of the order of a day or two (considering both gradient-curvature and $\mathbf{E} \times \mathbf{B}$ drifts) [*Chisham*, 1996]. These O^+ ions could have originated from the substorm particle injection at 0200 UT on May 12, 1988. However, as a result of the energy dispersion of injected ions, higher energy ions would be expected to reach the wave generation region before lower energy ions. Figure 7c suggests that for this event, ~15 keV O^+ ions would be needed at the start of the event, and ~20 keV O^+ ions would be needed at the end of the event. This is opposite to the expected energy dispersion and hence argues against this interpretation.

However, the possibility does exist that this wave is a fundamental standing mode wave. In this case, particles satisfying the $N = 0$ drift resonance condition will be in resonance with the wave. This criterion is satisfied by ions with a drift speed which matches the azimuthal phase speed of the wave, $V_{\phi-\text{phase}}$. Figure 7d displays the energy of all ions satisfying the $N = 0$ instability criterion. Ions with energies in the range 160 - 200 keV match the criterion in the region of interest. These particles have drift periods of the order of a couple of hours. It is possible that H^+ and/or O^+ ions of this energy were injected into the magnetosphere during the isolated substorm which occurred some hours earlier and drifted round the Earth more than once before being responsible for the wave excitation. The variations in ω and m during the event also match closely those that would be expected to result from the energy dispersion of these drifting ions. A drift resonance interaction with ions is therefore a likely scenario for the wave excitation.

4. Summary

In this paper we have used unique data analysis techniques to study an unusual large-m Pc5 ULF wave observed by SAMNET within the plasmasphere. The potential ambiguity in m-value magnitude has been eliminated by the comparison of m values between more than one set of station pairs in a longitudinal chain. Complex demodulation analysis of the Pc5 event produced the temporal variations in the wave period/frequency and m value leading to a characterization of the azimuthal dispersion properties of the wave. No firm conclusions regarding the generation mechanism of this wave can be made without knowledge of the harmonic mode of the wave and the stability of the local energetic ion distributions. However, a possible scenario is that the wave originated from a drift-bounce resonance interaction with energetic ions at the inner edge of the ring current.

Acknowledgments. SAMNET is deployed and operated by the University of York. GC was supported in part by a PPARC research grant, and IRM was supported by a PPARC fellowship.

Michel Blanc thanks Donald R. McDiarmid and Réjean Grard for their assistance in evaluating this paper.

References

Allan, W., E.M. Poulter, and E. Nielsen, STARE observations of a Pc5 pulsation with large azimuthal wave number, *J. Geophys. Res., 87*, 6163, 1982.

Allan, W., E.M. Poulter, K.-H. Glassmeier, and E. Nielsen, Ground magnetometer detection of a large-m Pc5 pulsation observed with the STARE radar, *J. Geophys. Res., 88*, 183, 1983.

Anderson, B.J., M.J. Engebretson, S.P. Rounds, L.J. Zanetti, and T.A. Potemra, A statistical study of Pc 3-5 pulsations observed by the AMPTE/CCE magnetic fields experiment, 1, Occurrence distributions, *J. Geophys. Res., 95*, 10,495, 1990.

Arthur, C.W., and R.L. McPherron, The statistical character of Pc4 magnetic pulsations at synchronous orbit, *J. Geophys. Res., 86*, 1325, 1981.

Banks, R.J., Complex demodulation of geomagnetic data and the estimation of transfer functions, *Geophys. J. R. Astron. Soc., 43*, 87, 1975.

Barfield, J.N., and R.L. McPherron, Statistical characteristics of storm-associated Pc5 micropulsations observed at the synchronous equatorial orbit, *J. Geophys. Res., 77*, 4720, 1972.

Barfield, J.N., R.L. McPherron, P.J. Coleman Jr., and D.J. Southwood, Storm-associated Pc5 micropulsation events observed at the synchronous equatorial orbit, *J. Geophys. Res., 77*, 143, 1972.

Beamish, D., H.W. Hanson, and D.C. Webb, Complex demodulation applied to Pi2 geomagnetic pulsations, *Geophys. J. R. Astron. Soc., 58*, 471, 1979.

Bingham, C., M.D. Godfrey, and J.W. Tukey, Modern techniques of power spectrum estimation, *IEEE Trans. Audio Electroacoust., 15*, 56, 1967.

Chen, L., and A. Hasegawa, A theory of long-period magnetic pulsations, 1, Steady state excitation of field line resonance, *J. Geophys. Res., 79*, 1024, 1974.

Chisham, G., Giant pulsations: An explanation for their rarity and occurrence during geomagnetically quiet times, *J. Geophys. Res., 101*, 24,755, 1996.

Chisham, G., and D. Orr, A statistical study of the local time asymmetry of Pc5 ULF wave characteristics observed at midlatitudes by SAMNET, *J. Geophys. Res., 102*, 24,339, 1997.

Chisham, G., D. Orr, M.J. Taylor, and H. Lühr, The magnetic and optical signature of a Pg pulsation, *Planet. Space Sci., 38*, 1443, 1990.

Chisham, G., D. Orr, and T.K. Yeoman, Observations of a giant pulsation (Pg) across an extended array of ground magnetometers and on auroral radar, *Planet. Space Sci., 40*, 953, 1992.

Chisham, G., I.R. Mann, and D. Orr, A statistical study of giant pulsation latitudinal polarization and amplitude variation, *J. Geophys. Res., 102*, 9619, 1997.

Grant, I.F., D.R. McDiarmid, and A.G. McNamara, A class of high-*m* pulsations and its auroral radar signature, *J. Geophys. Res., 97*, 8439, 1992.

Green, C.A., Giant pulsations in the plasmasphere, *Planet. Space Sci., 33*, 1155, 1985.

Hanson, H.W., D.C. Webb, and D. Beamish, A high resolution study of continuous pulsations in the European sector, *Planet. Space Sci., 27*, 1371, 1979.

Hasegawa, A., Drift mirror instability in the magnetosphere, *Phys. Fluids, 12*, 2642, 1969.

Hillebrand, O., J. Munch, and R.L. McPherron, Ground-satellite correlative study of a giant pulsation event, *J. Geophys., 51*, 129, 1982.

Hughes, W.J., The effect of the atmosphere and ionosphere on long period magnetic pulsations, *Planet. Space Sci., 22*, 1157, 1974.

Hughes, W.J., and R.J.L. Grard, A second harmonic geomagnetic field line resonance at the inner edge of the plasma sheet: GEOS1, ISEE1, and ISEE2 observations, *J. Geophys. Res., 89*, 2755, 1984.

Hughes, W.J., and D.J. Southwood, The screening of micropulsation signals by the atmosphere and ionosphere, *J. Geophys. Res., 81*, 3234, 1976a.

Hughes, W.J., and D.J. Southwood, An illustration of modification of geomagnetic pulsation structure by the ionosphere, *J. Geophys. Res., 81*, 3241, 1976b.

Hughes, W.J., R.L. McPherron, and J.N. Barfield, Geomagnetic pulsations observed simultaneously on three geostationary satellites, *J. Geophys. Res., 83*, 1109, 1978.

Hughes, W.J., R.L. McPherron, J.N. Barfield, and B.H. Mauk, A compressional Pc4 pulsation observed by three satellites in geostationary orbit near local midnight, *Planet. Space Sci., 27*, 821, 1979.

Kivelson, M.G., and D.J. Southwood, Resonant ULF waves: A new interpretation, *Geophys. Res. Lett., 12*, 49, 1985.

Kivelson, M.G., and D.J. Southwood, Coupling of global magnetospheric MHD eigenmodes to field line resonances, *J. Geophys. Res., 91*, 4345, 1986.

Kokubun, S., K.N. Erickson, T.A. Fritz, and R.L. McPherron, Local time asymmetry of Pc 4-5 pulsations and associated particle modulations at synchronous orbit, *J. Geophys. Res., 94*, 6607, 1989.

Lennartsson, W., and R.D. Sharp, A comparison of the 0.1 - 17 keV/e ion composition in the near equatorial magnetosphere between quiet and disturbed conditions, *J. Geophys. Res., 87*, 6109, 1982.

Lin, N., R.L. McPherron, M.G. Kivelson, and D.J. Williams, An unambiguous determination of the propagation of a compressional Pc5 wave, *J. Geophys. Res., 93*, 5601, 1988.

Mann, I.R., G. Chisham, and S.D. Bale, Multisatellite and ground-based observations of a tailward propagating Pc5 magnetospheric waveguide mode, *J. Geophys. Res., 103*, 4657, 1998.

Orr, D., and D.C. Webb, Statistical studies of geomagnetic pulsations with periods between 10 and 70 seconds and their relationship to the plasmapause region, *Planet. Space Sci., 23*, 1169, 1975.

Poulter, E.M., W. Allan, E. Nielsen, and K.-H. Glassmeier, STARE radar observations of a Pg pulsation, *J. Geophys. Res., 88*, 5668, 1983.

Pu, Z.-Y., and M.G. Kivelson, Kelvin-Helmholtz instability at the magnetopause: Energy flux into the magnetosphere, *J. Geophys. Res., 88*, 853, 1983.

Samson, J.C., Three-dimensional polarization characteristics of high-latitude Pc5 geomagnetic micropulsations, *J. Geophys. Res., 77*, 6145, 1972.

Sharp, R.D., W. Lennartsson, and R.J. Strangeway, The ionospheric contribution to the plasma environment in near-Earth space, *Radio Sci., 20*, 456, 1985.

Southwood, D.J., Some features of field line resonances in the magnetosphere, *Planet. Space Sci., 22*, 483, 1974.

Southwood, D.J., A general approach to low-frequency instability in the ring current plasma, *J. Geophys. Res., 81*, 3340, 1976.

Southwood, D.J., J.W. Dungey, and R.J. Etherington, Bounce resonant interaction between pulsations and trapped particles, *Planet. Space Sci., 17*, 349, 1969.

Takahashi, K., P.R. Higbie, and D.N. Baker, Azimuthal propagation and frequency characteristic of compressional Pc5 waves observed at geostationary orbit, *J. Geophys. Res., 90*, 1473, 1985.

Takahashi, K., R.W. McEntire, A.T.Y. Lui, and T.A. Potemra, Ion flux oscillations associated with a radially polarized transverse Pc5 magnetic pulsation, *J. Geophys. Res., 95*, 3717, 1990.

Takahashi, K., N. Sato, J. Warnecke, H. Lühr, H.E. Spence, and Y. Tonegawa, On the standing wave mode of giant pulsations, *J. Geophys. Res., 97*, 10,717, 1992.

Walker, A.D.M., R.A. Greenwald, A. Korth, and G. Kremser, STARE and GEOS2 observations of a storm time Pc5 ULF pulsation, *J. Geophys. Res., 87*, 9135, 1982.

Yeoman, T.K., Substorm associated pulsations: A study of plasmaspheric cavity resonance, midlatitude polarization and geostationary orbit signatures, D. Phil. thesis, Univ. of York, York, England, 1988.

Yeoman, T.K., D.K. Milling, and D. Orr, Pi2 pulsation polarisation patterns on the U.K. Sub-Auroral Magnetometer Network (SAMNET), *Planet. Space Sci., 38*, 589, 1990.

G. Chisham, British Antarctic Survey, Natural Environment Research Council, High Cross, Madingley Road, Cambridge CB3 0ET, England, U.K. (gchi@bas.ac.uk)

I.R. Mann, Department of Physics, University of York, Heslington, York YO10 5DD, England, U.K. (ian@aurora.york.ac.uk)

(Received November 16, 1998; revised January 27, 1999; accepted March 9, 1999.)